NMR Evidence for Triple-$\vec{q}$ Multipole Structure in NpO_2

Y. Tokunaga,[1] Y. Homma,[2] S. Kambe,[1] D. Aoki,[2] H. Sakai,[1] E. Yamamoto,[1] A. Nakamura,[1] Y. Shiokawa,[1,2] R. E. Walstedt,[1] and H. Yasuoka[1]

[1]*ASRC, Japan Atomic Energy Research Institute, Tokai, Ibaraki 319-1195, Japan*
[2]*IMR Tohoku University, 2145-2 Narita Oarai Higashiibaraki Ibaraki 311-1313, Japan*

(Received 19 November 2004; published 7 April 2005)

In order to elucidate the nature of the exotic ordered phase of NpO_2 below $T_0 = 26$ K, we have initiated the first ^{17}O-NMR measurements on this system. From the ^{17}O-NMR spectrum, the occurrence of two inequivalent oxygen sites has been confirmed below T_0. It has also been shown that the characteristic features of the hyperfine interaction at the oxygen sites are well explained by invoking a hyperfine interaction with field-induced antiferromagnetic moments which appear as a result of the triple-$\vec{q}$ antiferroquadrupolar order. The NMR findings strongly support the occurrence of the longitudinal triple-$\vec{q}$ multipole structure in NpO_2.

DOI: 10.1103/PhysRevLett.94.137209 PACS numbers: 75.25.+z, 76.60.–k

The low-temperature phase transition in NpO_2 has attracted much attention as a promising candidate for a new class of phase transitions associated with octupolar degrees of freedom [1,2]. This transition was originally discovered through specific heat and magnetic susceptibility measurements, which appeared to suggest a Néel transition to an antiferromagnetic (AFM) ordered state at $T_0 = 26$ K [3,4]. However, such a magnetic dipole ordering has been unambiguously ruled out by both neutron elastic scattering [5] and Mössbauer spectroscopy [6]. The upper limit on the ordered magnetic moments set by the Mössbauer experiments is $\mu_0 \leq 0.01\mu_B$/Np. Recently, Paixão *et al.* have performed resonant x-ray scattering (RXS) measurements and observed superlattice peaks signaling the occurrence of triple-$\vec{q}$ antiferroquadrupolar (AFQ) long-range order below T_0 [2]. They have pointed out, further, that the AFQ order observed could be driven by primary antiferro-octupolar (AFO) order of Γ_5 symmetry, since the AFQ order alone cannot successfully explain the observed saturation behavior of the susceptibility at low T [7], or the breaking of time reversal invariance observed with muon spin rotation (μSR) [8]. Up to now, however, no direct evidence for a triple-$\vec{q}$ magnetic structure has been reported.

Theoretically, the possibility of AFO order in NpO_2 was proposed initially by Santini and Amoretti [1]. Sakai *et al.* have recently derived the hyperfine interaction between multipolar moments and neighboring nuclear spins assuming the existence of triple-$\vec{q}$ AFO order, and have discussed the possibility of identifying the AFO moments using NMR [9]. More recently, multipole interactions on an fcc lattice have been derived from microscopic calculations based on the j-j coupling scheme by Kubo and Hotta [10]. They have found that the longitudinal triple-$\vec{q}$ AFO order ground state is realized in NpO_2 through the combined effects of multipole interactions and anisotropy of the Γ_5 moment.

In general, multipole order is hard to detect by conventional means. However, direct observation by NMR is possible in principle through hyperfine (HF) interactions with nuclear spins. Indeed, the ^{11}B-NMR in CeB_6 has been used to observe the HF interaction between the B nuclear spins and field-induced AFO moments in this system's AFQ order state [11–13].

In this Letter, we present the first NMR study of NpO_2. From the ^{17}O-NMR spectrum, we have confirmed the occurrence of two inequivalent oxygen sites below T_0. We also show that the temperature and field dependence of the ^{17}O NMR spectrum are well explained by invoking a HF interaction with field-induced AFM moments which appear as a result of the longitudinal triple-$\vec{q}$ AFQ order. These NMR results strongly support the occurrence of triple-$\vec{q}$ multipole structure in NpO_2.

The powder sample used in our ^{17}O NMR was prepared by oxidizing Np metal powder in O_2 gas containing 28 at. % ^{17}O. X-ray diffraction patterns confirmed a single-phase, cubic fluorite NpO_2 structure for our sample. Magnetic susceptibility measurements were found to reproduce Curie-Weiss behavior with a phase transition at $T_0 = 26$ K, as reported previously. The ^{17}O NMR measurements were carried out using a superconducting magnet and a phase coherent, pulsed spectrometer.

Figure 1 shows the temperature dependence of the field-sweep spectra obtained at resonant frequencies of (a) 15.4 MHz and (b) 59.2 MHz, respectively. The narrow, symmetric spectrum shown (30 K) has been obtained in the paramagnetic state. This indicates that there is no quadrupole splitting and no appreciable anisotropic NMR shift at the O sites, reflecting their cubic point symmetry above T_0. On the other hand, the spectrum in the ordered state gradually broadens with decreasing temperature. The spectra at the lower frequency [Fig. 1(a)] show a two-peak structure: one peak gradually broadens with decreasing temperature, while the other retains a narrow width while shifting to a higher field. The splitting of the spectrum strongly suggests the occurrence of two inequivalent O sites below T_0. By fitting the spectrum tentatively to a double Gaussian function, we obtained the ratio of the

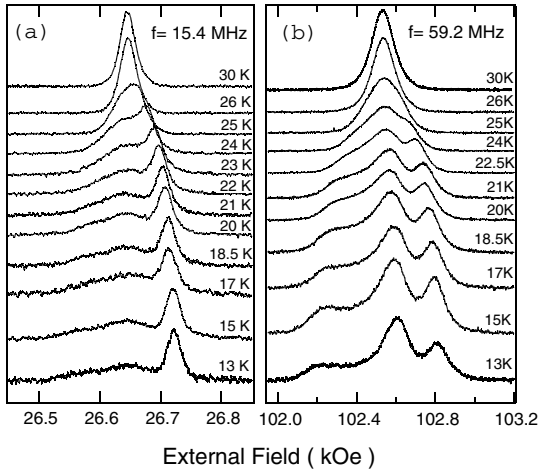

FIG. 1. The temperature dependence of the ^{17}O NMR spectra obtained at the resonant frequencies of (a) 15.4 MHz and (b) 59.2 MHz, respectively.

signal intensities to be 1:3 for the narrow and broad peaks, respectively, which is nearly T independent below T_0. This value indicates that $1/4$ of the oxygen sites are in a different microscopic environment from the other $3/4$ of the oxygen sites. Hereafter, we will denote the former sites as O(1) sites and the latter sites as O(3) sites, respectively. Inequivalent oxygen environments are also suggested by contrasting T_1 values obtained for the different peaks.

The spectra at the higher frequency [Fig. 1(b)] broaden markedly and show rather complicated structure at low temperature. The line shape is, however, well reproduced by the sum of two powder-pattern spectra characteristic of NMR in a powder sample. When a nucleus is in an environment of axial symmetry, the HF interaction produces an NMR shift $K(\theta) = K_{\rm iso} + K_{\rm ai}(3\cos^2\theta - 1)$, where $K_{\rm iso}$ and $K_{\rm ai}$ are the isotropic and anisotropic shift parameters, respectively, and θ is the angle between the local symmetry axis and the applied field H. In a powder sample, the observed spectrum includes contributions from all crystal orientations in a characteristic ''powder-pattern'' line shape. In the absence of other sources of broadening, the powder pattern shows a peak at $K_\perp = K_{\rm iso} - K_{\rm ai}$ and a shoulder at $K_\parallel = K_{\rm iso} + 2K_{\rm ai}$, so that the width is given by $\Delta = K_\parallel - K_\perp = 3K_{\rm ai}$. However, in order to compare this theoretical shape with experimental data, we have to take into account other sources of broadening, such as domain walls, radiation damage, electric quadrupole effects, etc. A simple way to model these effects is to take a convolution with a Gaussian or Lorentian broadening function of width δ. If $f(x)$ is the theoretical powder pattern and $g(y)$ the broadening function, the resulting envelope will be $F(y) = \int_{-\infty}^{+\infty} f(x)g(x-y)dx$. In Fig. 2(a), we show an example of calculated line shapes along with experimental data, where the dotted lines show two theoretical powder patterns $f(x)$ for the O(1) and the O(3) sites, and the solid lines show the respective envelopes $F(y)$ which results from Gaussian

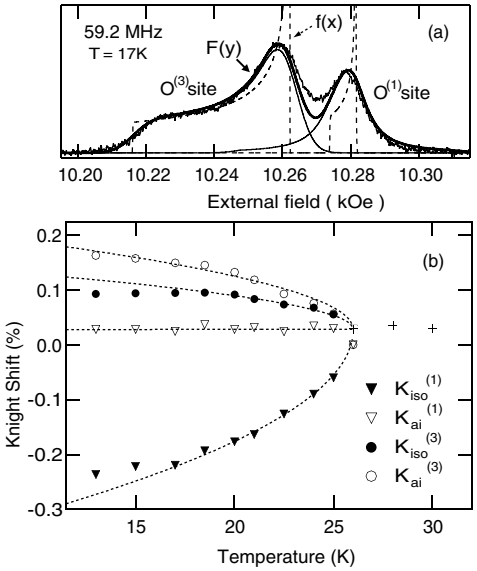

FIG. 2. (a) A example of the spectrum analysis. The dotted lines show two theoretical powder-pattern $f(x)$ for the O(1) and the O(3) sites, and the solid line shows their resulting envelopes $F(y)$ after weighting the symmetric broadening. (b) The T dependence of $K_{\rm iso}$ and $K_{\rm ai}$.

broadening. Further examples of calculated spectra are shown in Fig. 3. From this analysis, we can extract values of $K_{\rm iso}$, $K_{\rm ai}$, and δ for the O(1) and O(3) sites, separately.

T dependences of $K_{\rm iso}$ and $K_{\rm ai}$ so obtained are shown in Fig. 2(b). In the ordered state, we have obtained $|K_{\rm iso}| \gg |K_{\rm ai}|$ for the O(1) site, while $|K_{\rm iso}| \leq |K_{\rm ai}|$ for the O(3) site, respectively. This indicates that the HF coupling is almost isotropic at the O(1) site, while it is anisotropic at the O(3)

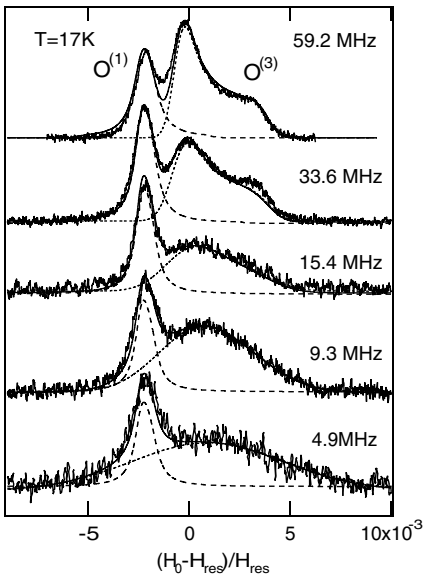

FIG. 3. The frequency dependence of spectra at $T = 17$ K. The solid and dotted lines show the results of the fittings (see in text).

site. It is also remarkable that the sign of the K_{iso} is negative for the O(1) site, while the signs of the K_{iso} and K_{ai} are positive for the O(3) site. The opposite sign of the HF coupling between two O sites quite unusual, and thus important when we consider the origin of the HF interactions below T_0.

Next we discuss the frequency dependence of the NMR spectrum. Figure 3 shows spectra obtained at different frequencies and fields. Since the spectral width is expected to scale with the field, the data in Fig. 3 are shown normalized by H_{res}, i.e., a NMR shift-distribution format. In this plot, the symmetric peak for the O(1) site does not change its width or position at the different frequencies, indicating that the shift and broadening are both scaled to H_{res}. On the other hand, the spectrum for the O(3) site shows a successive change from the powder pattern at high frequency to a broad, symmetric peak at low frequency. We found that this frequency dependence is well reproduced by assuming a progressive increase of δ/H_{res}, without any variation of K_{iso} and K_{ai}, as shown by the solid and dotted lines in Fig. 3.

In Fig. 4, we plot the field dependence obtained for δ for the O(1) and O(3) sites. At the O(1) site, we find $\delta^{(1)} \cong \alpha H$, while δ at the O(3) site includes a constant part, i.e. $\delta^{(3)} \cong \delta_0 + \alpha' H$, where $\delta_0 \sim 60$ Oe from the intercept as $H \rightarrow 0$. The α terms, which occur for both the O(1) and O(3) sites, simply represent distributions in the NMR shift ΔK. On the other hand, the δ_0 term suggests the existence of another source of HF interactions which remains even at zero field.

In the normal state, NpO_2 crystallizes in the fluorite structure with the cubic space group (SG) $Fm\bar{3}m$. Within this SG, all the oxygen ions occupy equivalent positions (the 8*c* position). Therefore, the observation of two inequivalent O sites by NMR give microscopic evidence for the symmetry lowering in the ordered state. Since the type of phase transition is second order, the SG of the ordered state must belong to the subgroups of $Fm\bar{3}m$. Among the maximal subgroups of $Fm\bar{3}m$, only the $Pn\bar{3}m$ SG has two inequivalent O sites (one:cubic 2*a*, the other:tetragonal 6*d*) in a ratio of one to three, in agreement with our experimental findings. It should be noted that, if the *longitudinal* triple-$\vec{q}$ structure is realized in the ordered state as suggested by the RXS , the symmetry is lowered from $Fm\bar{3}m$ to this $Pn\bar{3}m$ SG without any structural distortion [2,14]. The inequivalent O sites do not appear in the *transverse* triple-$\vec{q}$ structure (the $Pa\bar{3}$ SG) observed in UO_2.

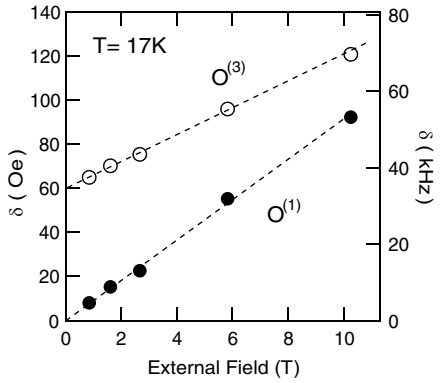

FIG. 4. The field dependence of δ for the O(1) and O(3) sites at $T = 17$ K.

In order to gain further insights into the multipole ordering state, we next investigate the microscopic origin of the HF interaction observed below T_0. Characteristic features of the HF interaction are: (1) it is proportional to the magnitude of the applied field, except for a small, constant broadening term at O(3) sites, (2) it appears only below T_0, (3) it shows the isotropic and anisotropic character at the O(1) and O(3) sites, respectively, and (4) it has opposite signs for the O(1) and O(3) sites. We show below that these characteristic features (1)–(4) are well explained by invoking a HF interaction with field-induced AFM moments which appear as a result of the triple-$\vec{q}$ AFQ order.

Ordinarily, the application of a magnetic field induces a uniform magnetization along the field, $M = \chi_0 H$. However, if the system exhibits AFQ order, an AFM moment can also be induced in conjunction with the AFQ order. As has been noted recently [9,15], if the triple-$\vec{q}$ structure of the AFQ moments is assumed, the AFM moments produce a static HF coupling at O sites given by

$$H_{hf} = -\gamma \mathbf{H} \cdot \left[\sum_i (\mathbf{1} + \mathbf{K}^{(1)}) \cdot \mathbf{I_i} + \sum_j (\mathbf{1} + \mathbf{K_j}^{(3)}) \cdot \mathbf{I_j} \right], \quad (1)$$

where i and j are summed over type (1) and (3) oxygen

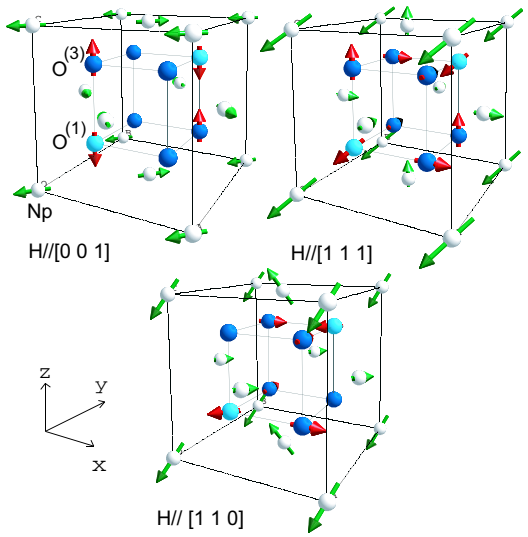

FIG. 5 (color online). The green arrows represent the field-induced AFM moments on Np sites appearing in cooperation with the longitudinal triple-$\vec{q}$ AFQ order and the magnetic field applied parallel to [0 0 1], [1 1 0], and [1 1 1] axes, respectively [9,15]. The red arrows show the classical dipolar field produced on O sites by the AFM moments on Np sites.

sites, respectively, and $\mathbf{K_i}$ and $\mathbf{K_j}^{(3)}$ are the corresponding shift tensors. $\mathbf{K}^{(1)}$ is an isotropic tensor of the form $-[K_{\mathrm{AF}}, K_{\mathrm{AF}}, K_{\mathrm{AF}}]$ and $\mathbf{K_j}^{(3)}$ has the form $[0, 0, K_{\mathrm{AF}}]$, where the nonzero component is permuted between (x, y, z) depending on the particular O(3) site. 1 is the unit tensor. Further, $K_{\mathrm{AF}} = A_0\chi_{\mathrm{AF}}$, where χ_{AF} is the induced AFM moment per unit of applied (cubic axis) field in the AFQ state, and A_0 is the corresponding coupling coefficient.

The forgoing shift mechanism is illustrated in Fig. 5, which shows the AFM moments expected to appear when a field is applied along the [0 0 1], [1 1 0], and [1 1 1] axes, respectively [15]. A simple calculation then gives nonzero values for the classical dipolar field at the O sites, as indicated by red arrows in the figure. These results are consistent with the symmetry-derived result given above, where the induced field is always along the applied field for the O(1) and lies along the axis of symmetry for the O(3) sites. Further, the shifts are expected to have opposite signs for the O(1) and O(3) cases, as is observed.

In the forgoing we have neglected the HF coupling with the uniform magnetization. However, this term will be small in NpO_2, because the tetrahedral symmetry around an O ion cancels the dipolar contribution from χ_0. This assumption is also supported by the small isotropic shift (~ -0.4 kOe$/\mu_B$) found in the paramagnetic state. Thus, the AFM shift dominates in the ordered state, in spite of the fact that $\chi_0 \gg \chi_{\mathrm{AF}}$.

The anisotropic HF field at the O(3) results in a powder-pattern spectrum on averaging over all the directions. Thus, the resulting width of the powder pattern Δ is related to χ_{AF} as $\Delta \cong A_0\chi_{\mathrm{AF}}$. If we adopt the coupling constant $A_0 = A_D = 4.2$ kOe$/\mu_B$ obtained from the dipole calculation and use the experimental result $\Delta = 3K_{ax}^{(3)} = 0.48\%$, we can estimate that $\chi_{\mathrm{AF}} \sim 1.2 \times 10^{-3}\mu_B$/kOe. This value, however, should be regarded as an upper limit, since one generally expects an enhancement of the HF coupling constant $A_0 > A_D$ owing to hybridization effects, etc. For example, we have obtained $A_0 \cong 4.3$ kOe$/\mu_B$ in the AFM ordered state of UO_2, which is about 2 times larger than $A_D \cong 2.4$ kOe$/\mu_B$ expected from a dipolar calculation [16].

In the argument above, we have considered only the HF interaction with the field-induced AFM moments in the ordered state. Although this AFM term is expected to give a major contribution in the HF mechanism, other types of HF interaction are also expected. Sakai *et al.* have suggested: (a) HF coupling with field-induced AFO moments, (b) quadrupole coupling with the field-induced AFQ, and (c) a higher order interaction due to the field-induced HF splitting [9]. The (a) term arises from secondary AFQ order, while the (b) and (c) terms arise directly from the primary AFO order. Therefore, observation of the (b) and (c) terms by means of NMR would be important for the identification of spontaneous AFO order in NpO_2. At the present stage, however, we could not resolve these contributions individually from the powder NMR spectrum. More detailed NMR studies in a single crystal sample are now in preparation.

Finally, we comment on the low-frequency line broadening observed for the O(3) site (the δ_0 term). This δ_0 term implies the existence of HF interactions which remain effective even at zero field. At zero field, however, the primary AFO order does not produce any HF field on the O sites owing to the T_d site symmetry around the O ions. On the other hand, the secondary AFQ order might possibly produce an electric field gradient at the O(3) site [9]. Therefore, one possible origin of the δ_0 term is this quadrupole interaction. This is, however, still uncertain, since we have no experimental evidence for such a quadrupole splitting up to now. The δ_0 term may also be of magnetic origin. Thus, HF interactions with "tiny-moment magnetism" induced by strains and/or defects are another possibility [1]. NMR studies on a single crystal sample will also help to resolve this point.

In conclusion, from the first NMR study of NpO_2, the occurrence of two inequivalent oxygen sites has been confirmed below T_0. It has also been shown that the temperature and field dependence of the ^{17}O NMR spectrum can be understood by considering an unconventional HF interaction between the ^{17}O nuclear spins and field-induced AFM moments arising from the longitudinal triple-$\vec{q}$ AFQ order. These NMR results give strong evidence for the occurrence of the longitudinal triple-$\vec{q}$ multipole structure in NpO_2.

The authors would like to thank O. Sakai, R. Shiina, T. Hotta, and K. Kubo for valuable discussions.

[1] P. Santini and G. Amoretti, Phys. Rev. Lett. **85**, 2188 (2000).
[2] J. A. Paixão *et al.*, Phys. Rev. Lett. **89**, 187202 (2002).
[3] D. W. Osborne *et al.*, J. Chem. Phys. **21**, 1884 (1953).
[4] J. W. Ross and D. J. Lam, J. Appl. Phys. **38**, 1451 (1967).
[5] R. Caciuffo *et al.*, Solid State Commun. **64**, 149 (1987).
[6] J. M. Friedt *et al.*, Phys. Rev. B **32**, 257 (1985).
[7] P. Erdös *et al.*, Physica B (Amsterdam) **102**, 164 (1980).
[8] W. Kopmann *et al.*, J. Alloys Compd. **271**, 463 (1998).
[9] O. Sakai *et al.*, J. Phys. Soc. Jpn. **74**, 457 (2005).
[10] K. Kubo and T. Hotta, Phys. Rev. B (to be published).
[11] M. Takigawa *et al.*, J. Phys. Soc. Jpn. **52**, 728 (1983).
[12] O. Sakai *et al.*, J. Phys. Soc. Jpn. **66**, 3005 (1997).
[13] R. Shiina *et al.*, J. Phys. Soc. Jpn. **67**, 941 (1998).
[14] D. Mannix *et al.*, Phys. Rev. B **60**, 15187 (1999).
[15] O. Sakai *et al.*, J. Phys. Soc. Jpn. **72**, 1534 (2003).
[16] K. Ikushima *et al.*, Phys. Rev. B **63**, 104404 (2001).